Available at www.sciencedirect.com

ScienceDirect

journal homepage: www.elsevier.com/locate/ijhydene

Catalytic hydrothermal gasification of cellulose and glucose

Zhen Fang[a,*], *Tomoaki Minowa*[b], *Chun Fang*[c], *Richard L. Smith, Jr*[d], *Hiroshi Inomata*[d], *Janusz A. Kozinski*[e]

[a]*Biomass Group, Xishuangbanna Tropical Botanical Garden, Chinese Academy of Sciences, 88 Xuefulu, Kunming, Yunnan province 650223, China*

[b]*Biomass Technology Research Center, National Institute of Advanced Industrial Science and Technology, 2-2-2 Hiro Suehiro, Kure, Hiroshima 737-0197, Japan*

[c]*AgWeatherNet Program, Washington State University, 24106 N Bunn Rd, Prosser, WA 99350, USA*

[d]*Department of Chemical Engineering, Research Center of Supercritical Fluid Technology, Tohoku University, Aoba-ku Aramaki Aza Aoba-04, Sendai 980-8579, Japan*

[e]*Department of Chemical Engineering, University of Saskatchewan, 57 Campus Drive, Saskatoon, Sask., Canada S7N 5A9*

ARTICLE INFO

Article history:
Received 28 May 2007
Received in revised form
26 September 2007
Accepted 28 November 2007
Available online 9 January 2008

Keywords:
Hydrothermal
Hydrogen
Cellulose
Glucose
Sub-and supercritical water
Gasification
Catalyst

ABSTRACT

An optical micro-reactor (50 nL), an autoclave (120 mL), and a flow reactor (11.3 mL) were used to study the catalytic hydrothermal gasification of cellulose and glucose. In the micro-reactor experiments, Ni catalyst had a low gasification rate, but 96 wt% rate (35 mol% H_2) was achieved in the autoclave when Ni/silica–alumina and cellulose were mixed well during slow heating to 350 °C (30 min). It was found from the micro-reactor that cellulose completely dissolved in water at 318 °C upon fast heating, and that Pt was the most active catalyst for glucose reactions. Gasification of glucose with Pt/γ-alumina catalyst was examined in flow experiments, where it was found that 67 wt% gasification rate (with up to 44 mol% H_2) could be obtained at 360 °C and 30 MPa.

1. Introduction

Water at a temperature and pressure that is near its critical point (CP; 374 °C, 22.1 MPa) is commonly referred to as hydrothermal water (HTW), which includes sub-critical water (SubW < CP) and supercritical water (SCW > CP). HTW behaves as a weakly polar solvent with both acidic and basic characters [1,2], and has the ability to hydrolyze and dissolve biomass. HTW can provide a homogeneous phase for biomass conversions [3,4]. Therefore, HTW has been used widely to gasify many different constituents of biomass, such as glucose [5–12], cellulose [4,6,10–15], lignin [12,14–17], organic wastes [12,14,18,19], starch [11,20,21] as well as actual biomass [10,21–25] without or with catalysts (e.g., ZrO_2, NaOH, KOH, Ni, Pt, CeO_2, Pd, RuO_2, Ru, $KHCO_3$ [4,6,9,10,12,14–17,19,20,25]). The following reactions can be considered to occur in HTW:

$$\text{Cellulose:}\quad (C_6H_{10}O_5)_n + nH_2O \rightarrow nC_6H_{12}O_6, \tag{1}$$

$$\text{Glucose:}\quad C_6H_{12}O_6 \rightarrow 6H_2 + 6CO, \tag{2}$$

$$\text{Water–gas shift (WGS):}\quad CO + H_2O \rightarrow H_2 + CO_2, \tag{3}$$

$$\text{Overall:}\quad (C_6H_{10}O_5)_n + 7nH_2O \rightarrow 12nH_2 + 6nCO_2. \tag{4}$$

*Corresponding author. Tel.: +86 871 5163360; fax: +86 871 5160916.
E-mail address: zhenfang@xtbg.ac.cn (Z. Fang).

0360-3199/$ - see front matter © 2007 International Association for Hydrogen Energy. Published by Elsevier Ltd. All rights reserved.
doi:10.1016/j.ijhydene.2007.11.023

According to Eqs. (1)–(4), theoretically, the gas produced from cellulose or glucose gasification can contain up to 66.7 mol% H_2. At moderately high temperatures (550−600 °C) and short reaction times in flow reactors, glucose can be 100% gasified with activated carbon or KOH catalyst with gas containing up to 60 mol% H_2 [5,7,19]. At lower temperatures (400−450 °C) and longer reaction times in batch reactors, 97% cellulose and 7.9% lignin can be gasified with RuO_2 (450 °C and 2 h) [14]. When Ru is used, 100% lignin can be gasified (400 °C and 3 h) [12]. In the batch gasification of cellulose with Ni (30 min), the gasification rate is very differently with 18% being obtained at 374 °C [23] and 84% being obtained at 350 °C [26].

Even though gasification technology is effective, little data concerning phase behavior of biomass decomposition with and without catalysts have been reported. Differences in the various cellulose gasification rates could be due to the phase behaviors or competing reaction kinetics that are controlled by mass transfer limitations. In this sense, a homogeneous reaction environment can be thought of as being advantageous for continuous chemical processing of water-insoluble biomass feedstocks. A homogeneous fluid can be obtained by flash-pyrolysis of biomass (wood), and subsequently reforming of the pyrolysis condensate in SCW to produce H_2 [27], which is a two-step (pyrolysis and hydrothermal) gasification process.

The purpose of this work is to produce H_2 rich gas from biomass in both batch and flow reactors. Cellulose and glucose were studied in a one-step hydrothermal process up to 400 °C with and without catalysts (Ni, Ru, and Pt). Three types of reactors were used: (i) a 50-nL optical micro-reactor, diamond anvil cell (DAC), (ii) a batch reactor (autoclave, 120 mL), and (iii) a flow reactor (11.3 mL). Catalyst activities, reactions, phase behaviors, and conditions for solubilizing cellulose were visually observed in the DAC during heating the {biomass/catalyst + water} system up to the supercritical region. These results were used to gasify glucose and cellulose in the autoclave (batch process) and in the flow reactor (continuous process).

2. Materials

Cellulose (microcrystalline powder; ~20 μm, 99.0% purity, DP = 229; Aldrich, Milwaukee, WI) and glucose (particles; >99.0% purity; Fluka, BioChemika) were used as representative biomass constituents. Aqueous solutions of 0.1- and 0.9-M glucose were made for the experiments in the DAC and flow reactor. Ni (powder; ~3 μm, 99.7% purity; Aldrich), Ru (sponge; ~20 mesh, 99.95% purity; Alfa Aesar, Ward Hill, MA) and Pt (1% Pt on γ-alumina powder; ~100 μm, Alfa Aesar) were used as the gasification catalysts in the DAC experiments. Ni catalyst used in the autoclave was prepared by crushing a commercial catalyst (Engelhard, NI-3288, ca. 50 wt% nickel on silica–alumina) to 60–200 mesh and treating it in a reducing atmosphere at 350 °C for 4 h. Pt pellets (0.5% Pt on $\frac{1}{8}$ in alumina pellets, AlfaAesar) were used as catalyst in the flow reactor.

3. Experimental approach

3.1. Reaction in DAC

An optical micro-reactor, Bassett-type [28] hydrothermal DAC was used for visual observations of {biomass + H_2O + catalyst} systems during heating process. The experimental setup and procedures are similar to our previously published works [4,29–32]. The reaction chamber (ca. 50 nL) consisted of a hole (500-μm i.d.) in an inconel gasket (250-μm thickness) and sealed by compression of two opposing diamond anvils. The micro-chamber was heated easily at slow and fast rates (0.1 to 20 °C/s) by two electric micro-heaters and can simulate reactions in batch and flow reactors at slow and fast heating rates. Temperature of the system was measured and recorded by a data acquisition unit (Strawberry Tree, Model DS-12-8-TC, Sunnyvale, CA). Water density (ρ) was adjusted by changing the size of argon gas bubbles introducing into the chamber and was calculated from the homogenization temperature (T_h), at which gas bubbles disappeared when heated.

Mixtures of {biomass + H_2O + catalyst} in the chamber were heated and observed under 110× magnification with a stereomicroscope (Olympus SZ11) with the images being recorded by a Panasonic 3-CCD camera (AW-E300). After completion of each experiment, the residues deposited on the lower and upper diamond anvils were analyzed by FT-IR microscopy (UMA 500, Bio-Rad, Cambridge, MA).

3.2. Gasification in an autoclave

Owing to micro-volume of the DAC, only microscopy techniques can be used to analyze products. Larger reactor is needed to get enough products for detailed analyses. A 120-mL autoclave (18-mL head space) was used to gasify cellulose. Cellulose (5 g), water (30 mL) and Ni catalyst (2 g) were loaded in the reactor. After being sealed, the autoclave with initial 3-MPa N_2 pressure was heated to 200−350 °C (4.3–16.5 MPa) at a heating rate of 0.18 °C/s and stirred by a magnetic stirrer. After reaching the desired temperature and holding time (0, 30 min, 1 h), the autoclave was cooled by cutting the electrical power. The gas volume was measured using a gas meter (Shinagawa-sheiki, W-NK-0.5B), and its composition was analyzed by gas chromatography (Shimadzu, GC-12A-TCD or GC-9A-FID). The reaction mixture was separated into three phases: (i) aqueous phase, (ii) oil phase (acetone-soluble), and (iii) water-insoluble fraction (residue). The aqueous phase was analyzed for total organic carbon (TOC) with a Yanaco TOC-8L analyzer and for glucose with a Shimadzu UV-160A absorption spectrometer. After freeze-drying, sugars in the aqueous phase (their trimethylsilyl derivatives) were analyzed with a GC (Hewlett-Packard, 5890A; CBP-10 column). Organic elements (C, H) of the oil and residue were analyzed by an elemental analyzer (AMCO NA-1500).

3.3. Gasification in the flow reactor

Continuous flow reactors are important for commercial applications of hydrothermal gasification technology. Stirred

tank, transpiring wall, and tubular flow reactors operating under hydrothermal and supercritical conditions have been reported in the literature [33,34]. In this work, we used a tubular flow reactor to check practical aspects and operation. The flow reactor used here was made of a $\frac{3}{8}$-inch 316-SS tube (11.3 mL; 400-mm length and 6.01-mm i.d.) loaded with 5-g Pt/Al_2O_3 pellets, which was heated by an electric tube furnace (F21100, Fisher) up to 400 °C. A high-pressure liquid chromatography pump (Model 510, Waters Associates, Milford, MA) was used to feed the prepared 0.1-M glucose solution. The solution was preheated in a $\frac{1}{16}$-inch 316-SS tube to 100 °C in 20 s and before being fed into the reactor. The reaction temperature (100−400 °C)in the center of the reactor tube, exit temperature at the end of the reactor and the preheated temperature were measured by K-type thermocouples (TJ36-Cain-116G-12, Omega). The pressure was controlled by a back-pressure regulator (Model: 54-2162D26, Tescom, MN) at 10–30 MPa. After leaving the reactor, effluent was rapidly quenched with a cooling water jacket to terminate the reaction. After reaction, products of three phases (gas, aqueous, and oil) were collected, separated, and analyzed as described similar to the above autoclave section.

4. Results and discussion

Three series of experiments have been conducted. The first series was carried out in the DAC. It focused on visual observations, activities of catalysts, phase behaviors, conditions for re-polymerization of glucose (residue formation) as well as complete dissolution of cellulose. These results were further used to gasify biomass to H_2 rich gas in batch (autoclave) and flow reactors. In the second series of experiments, gasification rates of insoluble cellulose with Ni catalyst were studied at low temperatures (⩽350 °C) and long reaction times (up to 1 h) in the autoclave. However, this batch-type process is not practical for commercial applications. Therefore, the third series of experiments were conducted in the flow reactor in order to produce H_2 continuously in short reaction times (e.g., 1 min). In the DAC, two types of phase behavior experiments were conducted: (i) slow heating rates (0.18 °C/s) (tests 1–2) and (ii) fast heating rates (9.5−14.5 °C/s) (tests 3–6) (Table 1). In the autoclave, two types of experiments were performed at the temperature and pressure conditions ranging from (200 °C, 4.3 MPa) to (350 °C, 16.5 MPa): (i) non-catalytic decomposition of cellulose and (ii) gasification of cellulose with Ni. In the flow reactor, a series of experiments was performed for continuous gasification of glucose with Pt from 100 to 400 °C.

Visual experimental conditions in the DAC are summarized in Table 1 (tests 1–6). Visual observations of the reactive phase behavior of cellulose and glucose are given in Fig. 1 (for slow heating tests 1–2), and Figs. 2–5 (for fast heating tests 3–6), respectively. Images and FT-IR spectra of the residues on lower and upper anvils are given in Figs. 6–8. Figs. 9–10 give carbon yields (%) for the four phase products (gas, oil, aqueous, and residue) from the cellulose decomposition in the autoclave without and with Ni catalyst. Carbon balances reported are based on the four phases. The gas compositions from both autoclave (Ni) and flow (Pt) gasification are given in Fig. 11. In the continuous Pt gasification of 0.1-M glucose, concentrations of glucose and TOC are given in Figs. 12 and 13, respectively. Results are discussed in detail in the below sections.

4.1. *Slow heating experiments*

Slow heating are widely used in batch processes. Biomass was catalytically gasified in HTW by slow heating (0.18 °C/s) to the reaction temperatures between 200 and 350 °C from room temperature. Total heating time to 350 °C was about 30 min. Ni was used as the catalyst because it has been shown to be effective for reforming biomass to hydrogen [26,35,36]. The DAC images are shown below.

4.1.1. *Visual observations (tests 1–2) with DAC*

In test 1, {cellulose + Ni + H_2O} with an argon gas bubble (Fig. 1A, a) was heated to 350 °C. Cellulose became yellow and transparent at 287 °C (Fig. 1A, b) and then dissolved at 293 °C maximum dissolution was reached at 320 °C (Fig. 1A, c and d). As temperature increased further to 350 °C, little change occurred for the non-dissolved cellulose (Fig. 1A, d and e).

Table 1 – Summary of experimental conditions in the diamond anvil cell

Experiments	Slow heating (0.18 °C/s)		Fast heating (9.5−14.5 °C/s)			
Sample Catalyst	Test 1 Cellulose Ni	Test 2 Glucose Ni	Test 3 Cellulose None	Test 4 Glucose Ni	Test 5 Glucose Ru	Test 6 Glucose Pt
Conditions						
Max. T (T_{max},°C)	350	350	319	400	400	400
Density of water at T_h (kg/m^3)	945	837	808	799	675	660
Average heating rate (°C/s)	0.18	0.18	11.1	9.5	14.4	14.5
T_h (homogenization T, °C)	118	223	244	250	317	323
Run time (s)[a]	1782	1811	26.5	39.0	26.0	26.0

[a] Heating time to the maximum temperature.

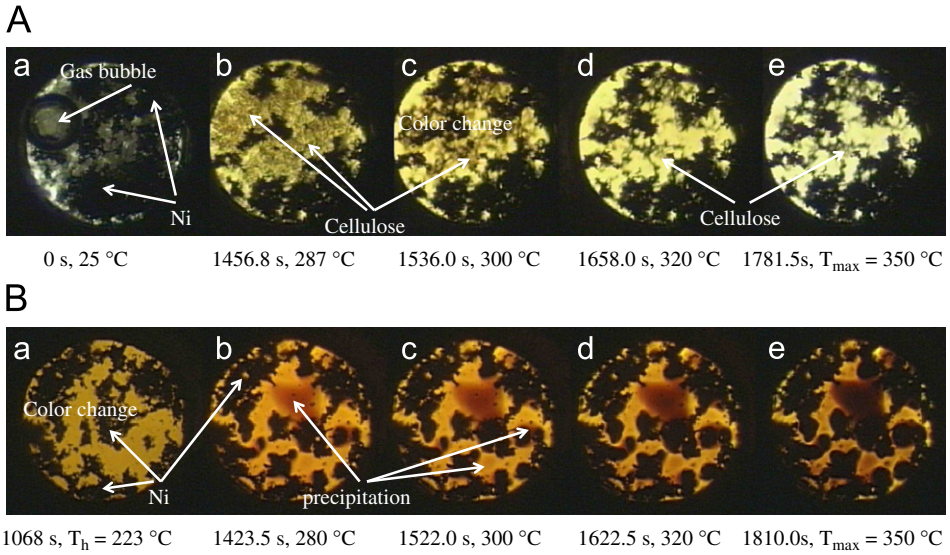

Fig. 1 – Visual observation of biomass for slow heating tests (Table 1; heating rate = 0.18 °C/s): (A) test 1: {cellulose + Ni + H_2O}, T_h = 118 °C, ρ = 945 kg/m³; (B) test 2: {glucose + Ni + H_2O}, T_h = 223 °C, ρ = 837 kg/m³.

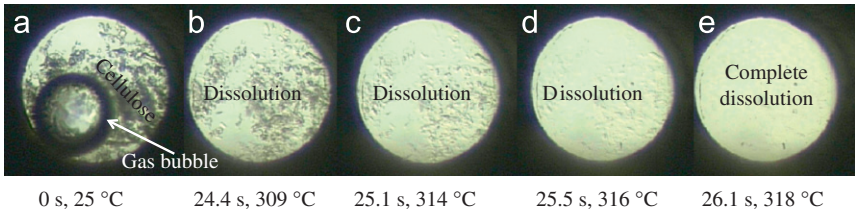

Fig. 2 – Visual observation of cellulose complete dissolution in water for fast heating test 3 (Table 1): heating rate = 11.1 °C/s, T_h = 244 °C, ρ = 808 kg/m³.

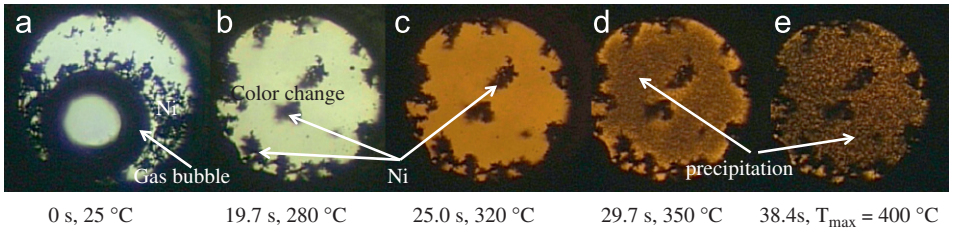

Fig. 3 – Visual observation of {glucose + Ni + H_2O} for fast heating test 4 (Table 1): heating rate = 9.5 °C/s, T_h = 250 °C, ρ = 799 kg/m³.

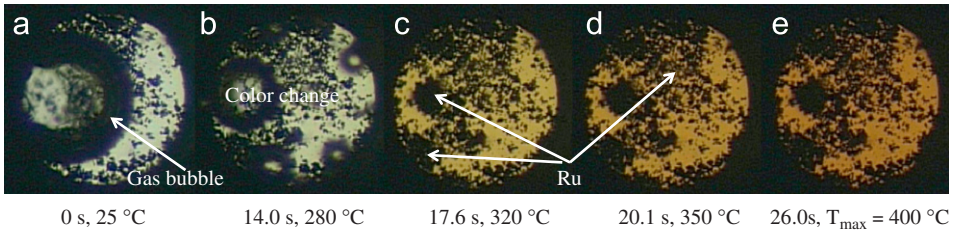

Fig. 4 – Visual observation of {glucose + Ru + H_2O} for fast heating test 5 (Table 1): heating rate = 14.4 °C/s, T_h = 317 °C, ρ = 675 kg/m³.

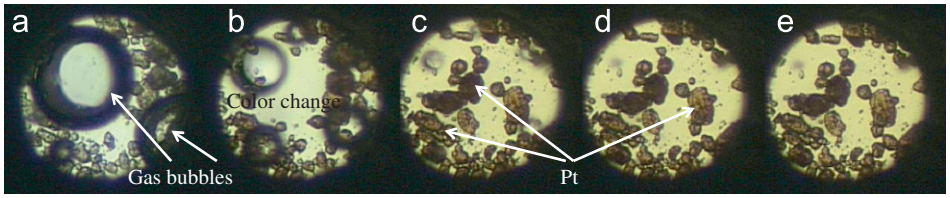

Fig. 5 – Visual observation of {glucose + Pt + H_2O} for fast heating test 6 (Table 1): heating rate = 14.5 °C/s, T_h = 323 °C, ρ = 660 kg/m^3.

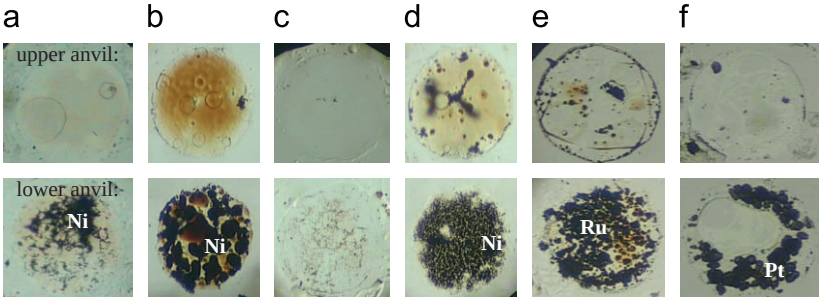

Fig. 6 – Residues on anvils for slow heating tests 1–2 (a,b) and fast heating tests 3–6 (c–f) (Table 1): top images for the upper anvil; bottom ones for the lower anvil.

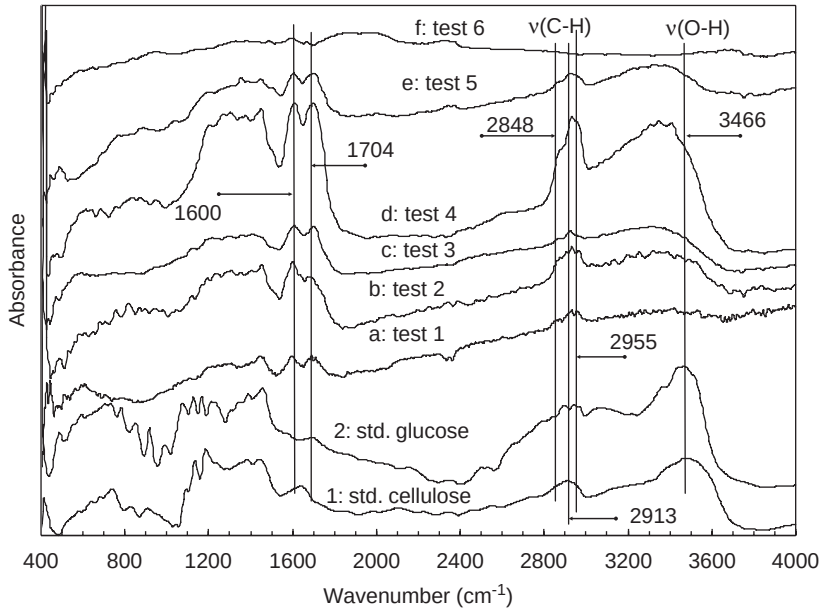

Fig. 7 – IR spectra for residues a–f from tests 1–6 on the lower anvil in Fig. 6.

After reaction, a thin film was formed on the upper diamond anvil, and non-dissolved residue and Ni particles remained on the lower anvil (Fig. 6a). IR results (Fig. 7, a: test 1) showed that the residue decomposed but still had a cellulose or glucose-like character as can be seen by a peak at 2913 cm^{-1} that is characteristic of cellulose, and three additional peaks at 1600, 1704 and 2955 cm^{-1}, whereas the peaks at 1704 and 2955 cm^{-1} are associated with glucose. The high residue yield (from re-polymerization) or low gasification rate, which was also confirmed in the batch tests with 18% gasification rate [23], was likely due to the heterogeneous reaction conditions, where non-dissolved cellulose had little chance to contact solid Ni particles. To check this possibility, glucose, which is water soluble and is the main product from hydrothermal reaction of cellulose [4,12,37], was selected in test 2 to observe its phase behavior during gasification process.

In test 2, 0.9-M glucose solution with Ni was heated to 350 °C at ρ = 837 kg/m^3. The loaded gas bubble disappeared at 223 °C (T_h) and the solution became yellow (Fig. 1B, a). At 280 °C, reddish oil-like product appeared (Fig. 1B, b) and this

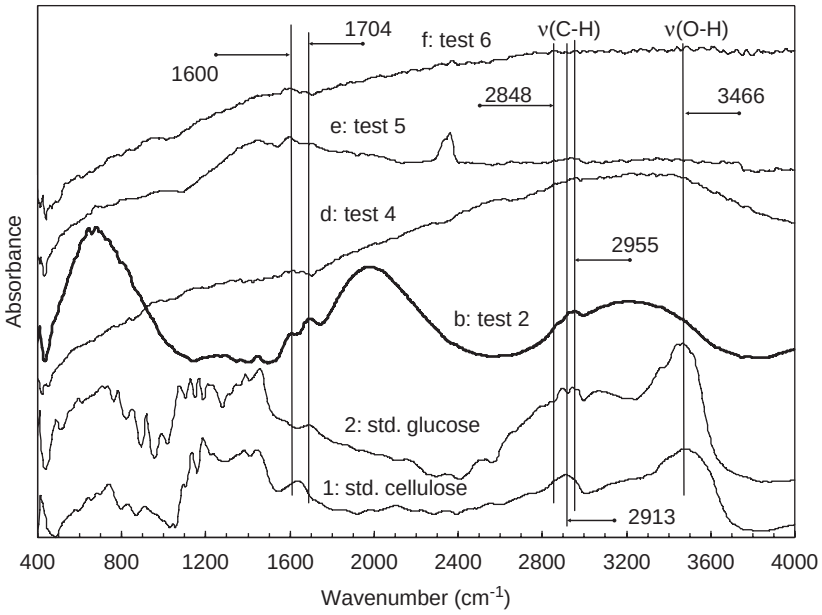

Fig. 8 – IR spectra for residues b, d–f from tests 2, 4–6 on the upper anvil in Fig. 6.

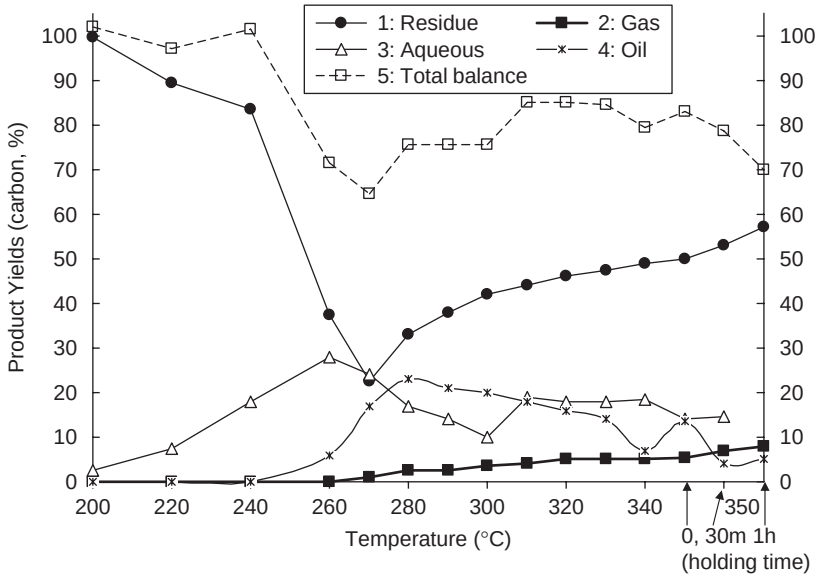

Fig. 9 – Product yields (carbon %) vs. temperature from non-catalytic decomposition of cellulose in the autoclave.

became black probably due to dehydration and condensation reactions [12] as the temperature approached to 350 °C (Fig. 1B, c and d). The oil-like product on both lower and upper anvils (Fig. 6b) was analyzed by FT-IR and was found to have a similar chemical structure to that in test 1 (Figs. 7–8, b).

In the above DAC gasification experiments, the by-products (solid residue and oil) yield was high thus gasification rate was low. One possible reason for this is that the limited phase contact between the heterogeneous catalyst Ni phase and the dissolved solutes. Another reason is that the catalytic activity of Ni powder without supports in the DAC is low as compared with Ni with supports due to their acidity/basicity [26]. The observed phase behavior shows that it is preferable to have agitation to promote mixing of cellulose with Ni/supports. Larger batch reactor (autoclave; 120 mL) was used for the gasification tests with Ni/supports in order to get enough quantities of products for detailed chemical analyses.

4.1.2. *Cellulose gasification in the autoclave*

First, non-catalytic decomposition of cellulose was studied with the autoclave at 200−350 °C as a blank experiment for the comparison with catalytic gasification. Gas products (carbon basis %; Fig. 9, curve 2) were produced from 260 °C and its yield gradually approached a maximum of 8% at 350 °C for holding 1 h. At low temperatures, CO_2 and CO (trace; because CO was converted to H_2 and CO_2 according to WGS reaction, Eq. (3)), were produced as primary gas products, and other hydrocarbon (HC) gases (CH_4, C_2H_4, and C_2H_6) and H_2 appeared at high temperatures. For the residue product

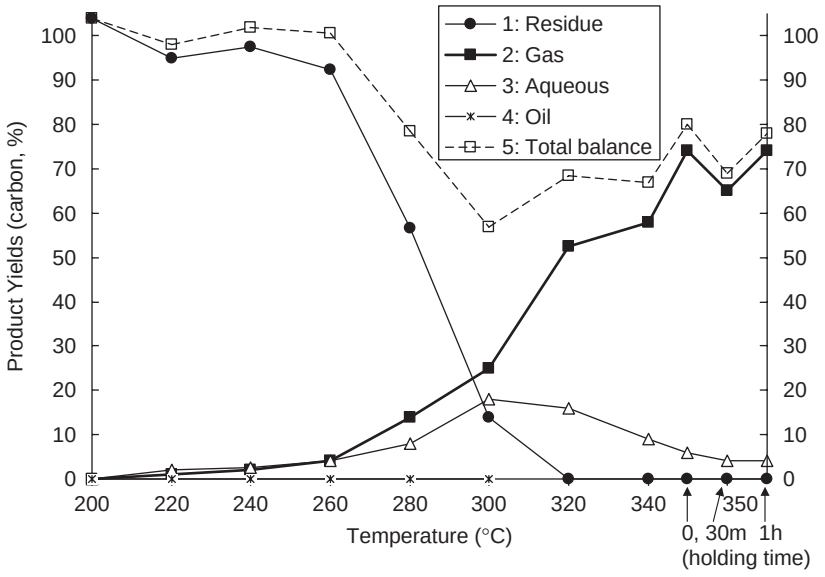

Fig. 10 – Product yields (carbon %) vs. temperature from catalytic gasification (Ni) of cellulose in the autoclave.

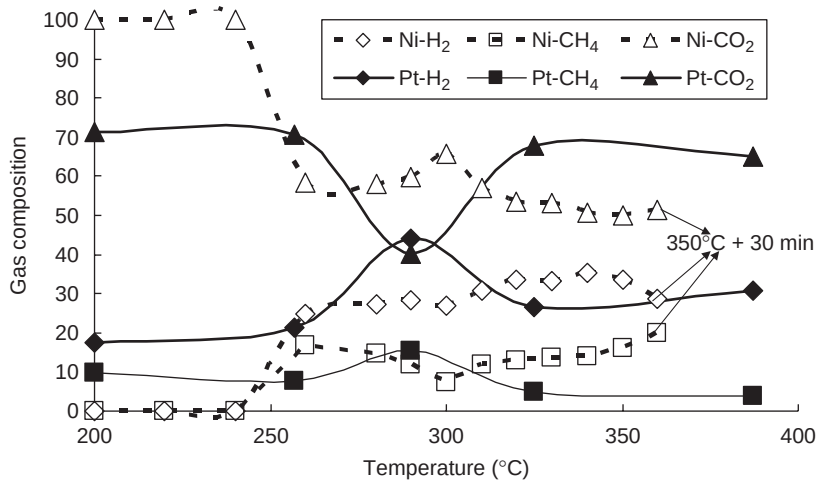

Fig. 11 – Gas composition vs. temperature from catalytic gasification. Dotted lines: cellulose with Ni in the autoclave; solid lines: glucose with Pt in the flow reactor at 3 ml/min flow rate (pump inlet).

(Fig. 9, curve 1), cellulose started decomposing slowly at 220 °C, and the residue yield decreased to 22.5% at 270 °C. After that, it climbed gradually to 50% at 350 °C and increased to 57% for holding 1 h at 350 °C. However, aqueous phase yield (Fig. 9, curve 3) increased smoothly up to the maximum of 28% (glucose yield = 17.5%) at 260 °C then it decreased to 10% at 300 °C and remained at around 14–19% until the temperature reached 350 °C. Other products, such as, yields of glucose, 5-(hydroxymethyl)furfural (HMF) and levoglucosan peaked at 260 °C and disappeared above 300 °C. For non-catalytic conditions, cellulose was first hydrolyzed to glucose, and subsequently decomposed to gas and solid residue.

Since gas yield was very low for the above non-catalytic decomposition, here Ni/silica–alumina catalyst was added to gasify cellulose during stirring and then the system was heated to temperatures between 200 and 350 °C. The residue yield (Fig. 10, curve 1) sharply decreased at above 260 °C and no residue was detected above 320 °C. The aqueous phase yield (Fig. 10, curve 3) peaked at 300 °C with a value of 18% and contained little glucose and then decreased to 4% at 350 °C for 1 h, in which no oil was produced. The gas yield (Fig. 9, curve 2) became perceptible from 220 °C and reached a maximum of 70% at 350 °C. In fact, at 350 °C, 96% cellulose was gasified if calculated by difference (with only 4% aqueous yield, and no residue or oil products). The lower starting gasification temperature (220 °C with Ni/silica–alumina vs. 260 °C without catalyst) is due to catalytic effect. Fig. 11 (dotted lines) shows that gas was composed mainly of CO_2, H_2, and CH_4. Below 240 °C, only CO_2 was produced while H_2 and CH_4 were appeared at 260 °C and decreased to the minimum values of 27 and 7 mol% at 300 °C, respectively. As temperature increased further to 350 °C and 30 min, H_2 reached the maximum of 35 mol% at 340 °C then decreased to 29 mol%, but CH_4 rose continuously to 20 mol%. The concentration of CO_2, H_2, and CH_4 at 350 °C, were 50, 34, and 16 mol%, respectively. The carbon balance was relatively low most

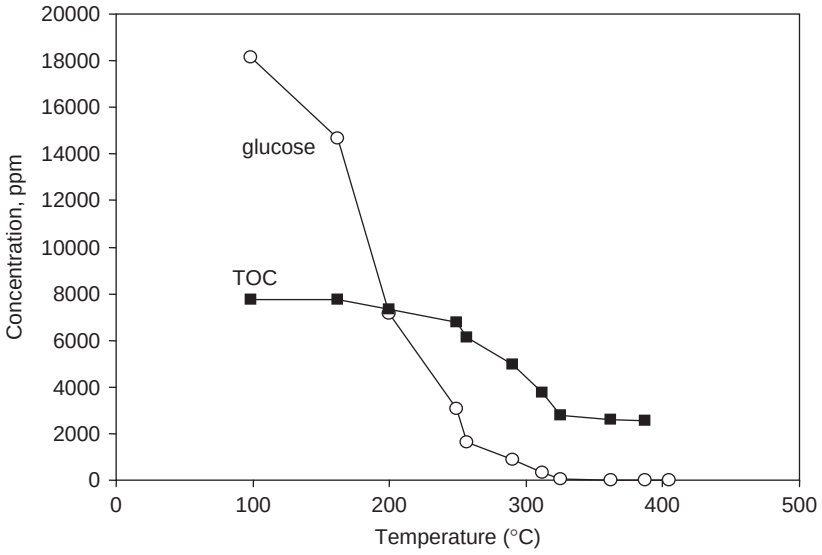

Fig. 12 – Concentrations of glucose and TOC vs. temperature from catalytic gasification (Pt) of 0.1-M glucose in the flow reactor at 3 ml/min flow rate (pump inlet).

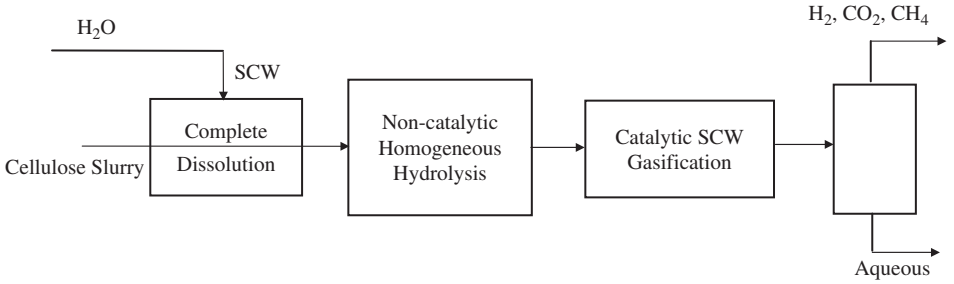

Fig. 13 – A simplified process for the cellulose gasification.

likely due to the gas loss during the collection at high pressures. Low H_2 concentration in the gas (35 mol%) as compared to the theoretical value of 66.7 mol% (Eq. (4)) is due to low reaction temperatures. When Ni catalyst was used, no HC ($>C_1$) gases were found because they would crack to CH_4 and H_2 according to the following reaction:

$$C_mH_n \rightarrow (n/2 - 2m)H_2 + mCH_4. \quad (5)$$

Observed decease in CH_4 and H_2 amounts between temperatures of 260 and 300 °C was likely due to less HCs being produced from cellulose decomposition for their production (Eq. (5)). Above 300 °C, H_2 rose according to the overall reaction (Eq. (4)) then decreased above 340 °C to produce CH_4 from CO_2 and H_2 via methanation according to the following reaction:

$$4H_2 + CO_2 \rightarrow CH_4 + 2H_2O. \quad (6)$$

The production of methane was confirmed by a separate series of experiments using only CO_2 and H_2 as starting samples [26]. Therefore, the composition changes of the three main gases (CO_2, H_2, and CH_4) can be explained by both Eqs. (5) and (6).

As shown in Fig. 10, cellulose could be effectively gasified to hydrogen-rich gas with Ni/silica–alumina catalyst at 350 °C. However, in the batch process long reaction times (e.g., at least 30 min) were required. Flow processes usually use at high heating rates and short reaction times (0.05–100 s) [34,37–39]. In the next section, high heating rates and slightly high temperatures (e.g., heated to 400 °C in 0.05−10 s) were studied in the DAC in an attempt to understand gasification yield.

4.2. *Fast heating experiments*

Biomass was visually studied in the DAC during fast heating to 400 °C at 9.5−14.5 °C/s to provide basic parameters for the flow reactor. Biomass then was studied in the flow process to continuously produce hydrogen.

4.2.1. *Visual observations (tests 3–6) with DAC*

In test 3 ($\rho = 808\,kg/m^3$; Fig. 2 and Table 1), {cellulose + H_2O} was rapidly heated to 400 °C at a heating rate of 11.1 °C/s. At 309 °C, cellulose started to dissolve, 1.7 s later, cellulose completely dissolved at 318 °C (Fig. 2, b–e). Solid residue (Fig. 6c) was obtained after cooled from 319 °C and analyzed by FT-IR. The residue was hydrolyzed but had a higher cellulose character than that in tests 1–2 because the stretching band for cellulose still remained as a single peak at 2913 cm^{-1}(Fig. 7, c: test 3). The visual appearance of the

liquid phase was strikingly different from those of the catalytic slow heating tests (Fig. 1A, 1B). In other research on conversion of cellulose at high heating rates, a high concentration glucose-oligomer solution was produced [37,39]. To study the possible gasification of such a hydrolyzed cellulose solution, we used glucose solutions as biomass model compound in the following catalytic experiments. Catalysts of Ni, Ru, and Pt are widely used in biomass gasification [12] and these were selected for the DAC tests to determine which catalyst is more active for the flow experiments.

In test 4 ($\rho = 799\,kg/m^3$; Fig. 3 and Table 1), Ni catalyst was used to gasify 0.9-M glucose during heating to 400 °C. The solution became light yellow color at 280 °C and orange color at 320 °C (Fig. 3, b and c). At 350 °C, numerous tiny particles precipitated and became black until 400 °C. After completion of the reaction, a yellow film formed on the upper anvil while solid particles were found on the lower anvil (Fig. 6d). IR spectrum (Fig. 7, d) showed that the particles were decomposed, but still had a strong glucose character due to strong stretching peaks that remained around $2913\,cm^{-1}$ and an additional peak at $1600\,cm^{-1}$. The film also had a glucose-like character (Fig. 8, d). In essence, the results showed that Ni catalyst was ineffective to promote gasification of glucose at the given conditions.

In test 5 ($\rho = 675\,kg/m^3$; Fig. 4 and Table 1), Ru particles were used. Similar to test 4, light yellow color appeared at 280 °C and gradually became orange color at 400 °C (Fig. 4, b–e). No solid residue produced and only some oil-like product remained on the anvils (Fig. 6e). IR spectra showed that the oil-like product still had a glucose character (Fig. 7, e). From these results, we concluded that Ru was more active than Ni catalyst for gasifying glucose.

In test 6 ($\rho = 660\,kg/m^3$; Fig. 5 and Table 1), Pt particles with γ-alumina support were used in order to increase catalytic activity. After a light yellow color appeared at 280 °C, the solution color changed slightly upon heating to 400 °C (Fig. 4, b–e). Little product remained on the anvils (Fig. 6f) and there were no peaks detected in the IR spectra (Figs. 7–8, f). In other words, most of the glucose was converted to probably volatile liquid or gas products. Considering the phase behavior, Pt/γ-alumina was found to be highly favorable for gasifying glucose and therefore, Pt/γ-alumina was selected for study under continuous conditions.

4.2.2. *Continuous gasification of glucose*

Fig. 12 shows how glucose concentration in the effluent changed with temperature after reaction with Pt catalyst in the flow apparatus. Glucose concentration decreased sharply above 100 °C and completely disappeared at 325 °C (Fig. 12). TOC in aqueous phase had a similar trend with temperature, and 67% carbon being converted to gas at 360 °C (Fig. 12). In Fig. 11 (solid lines), the main composition of the gas was CO_2, H_2, and CH_4, with up to 44-mol% H_2 being produced at 290 °C. Even as low as 200 °C, H_2 and CH_4 (17 and 10 mol%, respectively) were produced, which shows that Pt/γ-alumina is much more active than Ni/silica–alumina. There is a peak for both H_2 and CH_4 at 290 °C, which were produced by cracking HCs (Eq. (5)). However, little methanation reaction (Eq. (6)) occurred at high temperatures due to short reaction times.

Based on the above results, a simplified process can be proposed for the gasification (Fig. 13): First, cellulose can be rapidly heated to the supercritical region and subsequently completely dissolved into water. Homogeneous hydrolysis will occur to produce glucose and shorter cellulose oligomers. Then these products can be decomposed further to water-soluble products, and finally gasified with catalysts (Pt or others) or polymerized to solid residue without catalyst.

5. Conclusions

Biomass with Ni catalyst was very hard to be gasified at low temperatures (e.g., 350 °C) or short reaction times (e.g., 30 s) without good mixture and supports. But, 96 wt% cellulose could be gasified if {cellulose + Ni/silica–alumina + H_2O} was mixed well by a stirrer in the autoclave. Cellulose completely dissolves in water at 318 °C and subsequently undergoes homogeneous hydrolysis to glucose and oligomers when heated rapidly, which makes it possible to design a flow reactor to continuously gasify solubilized cellulose or glucose. In the DAC experiments, Pt was found to be the most active catalyst as compared with Ni and Ru catalysts. In the gasification of glucose with Pt in the flow reactor, a H_2 rich gas with 67-wt% gasification rate was obtained. DAC techniques are convenient to study the phase behavior, reactions, solubilization of biomass and catalyst activity at high pressure and temperature water. It is clear that hydrothermal gasification of biomass can be thoroughly studied through the novel combination of DAC, autoclave and flow experiments.

Acknowledgment

The author (ZF) wishes to acknowledge the financial support from Chinese Academy of Sciences (Rencai Yinjin program: 2 million Yuan).

REFERENCES

[1] Uematsu M, Franck EU. Static dielectric constant of water and steam. J Phys Chem Ref Data 1980;9(6):1291–306.
[2] Marshall WL, Franck EU. Ion product of water substance, 0–1000 °C, 1–10,000 bars new international formulation and its background. J Phys Chem Ref Data 1981;10(2):295–304.
[3] Bobleter O. Hydrothermal degradation of polymers derived from plants. Prog Polym Sci 1994;19:797–841.
[4] Fang Z, Minowa T, Smith Jr RL, Ogi T, Kozinski JA. Liquefaction and gasification of cellulose with Na_2CO_3 and Ni in subcritical water at 350 °C. Ind Eng Chem Res 2004;43(10):2454–63.
[5] Yu D, Aihara M, Antal Jr MJ. Hydrogen production by steam reforming glucose in supercritical water. Energy Fuel 1993;7:574–7.
[6] Watanabe M, Inomata H, Arai K. Catalytic hydrogen generation from biomass (glucose and cellulose) with ZrO_2 in supercritical water. Biomass Bioenergy 2002;22:405–10.
[7] Xu X, Matsumura Y, Stenberg J, Antal Jr MJ. Carbon-catalyzed gasification of organic feedstocks in supercritical water. Ind Eng Chem Res 1996;35:2522–30.
[8] Sinag A, Kruse A, Rathert J. Influence of the heating rate and type of catalyst on the formation of key intermediates and on

the generation of gases during hydropyrolysis of glucose in supercritical water in a batch reactor. Ind Eng Chem Res 2004;43(2):502–8.
[9] Hashaikeh R, Fang Z, Butler IS, Kozinski JA. Sequential hydrothermal gasification of biomass to hydrogen. Proc Combust Inst 2005;30:2231–7.
[10] Lu YJ, Guo LJ, Ji CM, Zhang XM, Hao XH, Yan QH. Hydrogen production by biomass gasification in supercritical water: a parametric study. Int J Hydrogen Energy 2006;31: 822–31.
[11] Williams PT, Onwudili J. Subcritical and supercritical water gasification of cellulose, starch, glucose, and biomass waste. Energy Fuel 2006;20:1259–65.
[12] Osada M, Sato T, Watanabe M, Shirai M, Arai K. Catalytic gasification of wood biomass in subcritical and supercritical water. Combust Sci Technol 2006;178:537–52.
[13] Kruse A, Henningsen T, Sinag A, Pfeiffer J. Biomass gasification in supercritical water: influence of the dry matter content and the formation of phenols. Ind Eng Chem Res 2003;42:3711–7.
[14] Izumizaki Y, Park KC, Tachibana Y, Tomiyasu H, Fujii Y. Organic decomposition in supercritical water by an aid of ruthenium (IV) oxide as a catalyst-exploitation of biomass resources for hydrogen production. Prog Nucl Energy 2005;47(1–4):544–52.
[15] Osada M, Sato T, Watanabe M, Adschiri T, Arai K. Low-temperature catalytic gasification of lignin and cellulose with a ruthenium catalyst in supercritical water. Energy Fuel 2004;18(2):327–33.
[16] Watanabe M, Inomata H, Osadab M, Sato T, Adschiri T, Arai K. Catalytic effects of NaOH and ZrO_2 for partial oxidative gasification of *n*-hexadecane and lignin in supercritical water. Fuel 2003;82:545–52.
[17] Osada M, Sato O, Arai K, Shirai M. Stability of supported ruthenium catalysts for lignin gasification in supercritical water. Energy Fuel 2006;20:2337–43.
[18] Xu X, Antal Jr MJ. Gasification of sewage sludge and other biomass for hydrogen production in supercritical water. Environ Prog 1998;17(4):215–20.
[19] Schmieder H, Abeln J, Boukis N, Dinjus E, Kruse A, Kluth M, et al. Hydrothermal gasification of biomass and organic wastes. J Supercritical Fluids 2000;17:145–53.
[20] D'Jesus P, Cristian Artiel C, Boukis N, Kraushaar-Czarnetzki B, Dinjus E. Influence of educt preparation on gasification of corn silage in supercritical water. Ind Eng Chem Res 2005;44:9071–7.
[21] D'Jesus P, Boukis N, Kraushaar-Czarnetzki B, Dinjus E. Gasification of corn and clover grass in supercritical water. Fuel 2006;85:1032–8.
[22] Antal Jr MJ, Allen SG, Schulman D, Xu X, Divilio RJ. Biomass gasification in supercritical water. Ind Eng Chem Res 2000;39:4040–53.
[23] Modell M. Gasification and liquefaction of forest products in supercritical water. In: Overend RP, Milne TA, Mudge LK, editors. Fundamentals of thermochemical biomass conversion. London, UK: Elsevier Applied Science; 1985. p. 95–119.
[24] Hashaikeh R, Fang Z, Butler IS, Hawari J, Kozinski JA. Hydrothermal dissolution of willow in hot compressed water as a model for biomass conversion. Fuel 2007;86:1614–22.
[25] Valenzuela MB, Jones CW, Agrawal PK. Batch aqueous-phase reforming of woody biomass. Energy Fuel 2006;20:1744–52.
[26] Minowa T, Ogi T. Hydrogen production from cellulose using a reduced nickel catalyst. Catal Today 1998;45:411–6.
[27] Penninger JML, Rep M. Reforming of aqueous wood pyrolysis condensate in supercritical water. Int J Hydrogen Energy 2006;31(11):1597–606.
[28] Bassett WA, Shen AH, Bucknum M, Chou I-M. A new diamond anvil cell for hydrothermal studies to 2.5 GPa and from-190 to 1200 °C. Rev Sci Instrum 1993;64(8):2340–5.
[29] Fang Z, Smith Jr RL, Inomata H, Arai K. Phase behavior and reaction of polyethylene terephthalate–water systems at pressures up to 173 MPa and temperatures up to 490 °C. J Supercritical Fluids 1999;15:229–43.
[30] Fang Z, Smith Jr RL, Inomata H, Arai K. Phase behavior and reaction of polyethylene in supercritical water at pressures up to 2.6 GPa and temperatures up to 670 °C. J Supercritical Fluids 2000;16:207–16.
[31] Smith Jr RL, Fang Z, Inomata H, Arai K. Phase behavior and reaction of nylon 6/6 in water at high temperatures and pressures. J Appl Polym Sci 2000;76(7):1062–73.
[32] Fang Z, Kozinski JA. Phase behavior and combustion of hydrocarbon-contaminated sludge in supercritical water at pressures up to 822 MPa and temperatures up to 535 °C. Proc Combust Inst 2000;28:2717–25.
[33] Shaw RW, Dahmen N. Destruction of toxic organic materials using supercritical water oxidation: current state of the technology. NATO Sci Ser, Ser E Appl Sci 2000;366:425–37.
[34] Fang Z, Xu S, Butler IS, Smith Jr RL, Kozinski JA. Destruction of decachlorobiphenyl using supercritical water oxidation. Energy Fuel 2004;18:1257–65.
[35] Sato T, Furusawa T, Ishiyama Y, Sugito H, Miura Y, Sato M, et al. Effect of water density on the gasification of lignin with magnesium oxide supported nickel catalysts in supercritical water. Ind Eng Chem Res 2006;45(2):615–22.
[36] Furusawa T, Sato T, Sugito H, Miura Y, Ishiyama Y, Sato M, et al. Hydrogen production from the gasification of lignin with nickel catalysts in supercritical water. Int J Hydrogen Energy 2007;32(6):699–704.
[37] Sasaki M, Fang Z, Fukushima Y, Adschiri T, Arai K. Dissolution and hydrolysis of cellulose in subcritical and supercritical water. Ind Eng Chem Res 2000;39:2883–90.
[38] Maharrey SP, Miller DR. Quartz capillary microreactor for studies of oxidation in supercritical water. AIChE J 2001;47(5):1203–11.
[39] Sasaki M, Kabyemela B, Malaluan R, Hirose S, Takeda N, Adschiri T, et al. Cellulose hydrolysis in subcritical and supercritical water. J Supercritical Fluids 1998;13(1–3):261–8.